Tracing source and mobility of arsenic and trace elements in a hydrosystem impacted by past mining activities (Morelos state, Mexico)

Aurélie Barats[1]*, Christophe Renac[1], Anna Maria Orani[1], Gaël Durrieu[2], Humberto Saint Martin[3], Maria Vicenta Esteller[4], Sofia Esperenza Garrido Hoyos[5]

**corresponding author : aurelie.barats@unice.fr*

[1] *Université Côte d'Azur, CNRS, Observatoire de la Côte d'Azur, IRD, Géoazur, 250 rue Albert Einstein, Sophia Antipolis 06560 Valbonne, France*

[2] *Université de Toulon, Aix Marseille Université, CNRS, IRD, Mediterranean Institute of Oceanography (MIO), UMR7294, 83041, Toulon Cedex 9, France*

[3] *Universidad Nacional Autónoma de México, Instituto de Ciencias Físicas, Cuernavaca, México*

[4] *Universidad Autonoma del Estado de Mexico, Instituto Interamericano de Teconología y Ciencias del Agua, Carretera Ixtlahuaca-Atlacomulco Km 14.5 San Cayetano Morelos, 50130, Toluca, México*

[5] *Instituto Mexicano de Tecnologia del Agua, Paseo Cuauhnahuac, Jiutepec, México*

Highlights

- Dissolved arsenate species are the main contaminant in waters.
- Suspended particles are a potential secondary source of water contamination.
- Organic contaminations occur in drinking waters.
- The As contamination may originate from the dissolution of sulfides by oxidation.
- TE contaminations in SPM due to oxi-hydroxides and sorption onto clays.

Key words: trace elements, arsenic, origin, water, sediment, mine

Abstract

The Sierra Huautla (Morelos State, Mexico) is a biological reserve with historical mines of Ag and Pb. In this area, waters used by inhabitants are contaminated by arsenic (As). An integrated environmental survey was realized both in waters and sediments to better constrain the source and the mobility of As and other trace elements. Two areas of interest were selected: (1) the Nexpa River ecosystem to determine the local geochemical background, and (2) the Huautla area, affected by past mining activities. This study allowed the definition of the local geochemical baseline in sediments or in waters, demonstrated uncontaminated by TE in the Nexpa area, except for As in the dissolved phase or for Cd in Suspended Particulate Matters (SPM). In the Huautla area, TE contents in water were higher than the World Health Organization (WHO) limits for Al, As and Mn in unfiltered waters, and only for As in the dissolved phase. Speciation analyses performed revealed arsenic to be present only as the toxic-inorganic arsenate species, As(+V). In SPM, Ag, As, Cd and Zn concentrations were higher than Sediment Quality Guidelines (SQG). The different geochemical indice (EF: 5, PLI: 3, EF: Igeo: 5-3) demonstrated that SPM were significantly contaminated and consistute an health risk for Huautla inhabitants exposed to As-contaminated waters and TE-rich SPM. The combination of mineralogy, chemistry, C and S stable isotopes with thermodynamic modeling indicate dissolutions of minerals from local geological formations, sorption-desorption phenomena from clays and oxy-hydroxides, and the weathering responsible for the transport of the TE-rich SPM (1.8 wt% for 17% of the total TE concentration). Moreover, the past mining activity would be a source of the contamination only for As in waters from flooded mines.

1. Introduction

Due to mining activities, the contamination of water, soil and riverine sediments is an environmental and health problem affecting many countries (Brumbaugh et al., 2013; de Souza et al., 2017; Parviainen et al., 2018; Zhang et al., 2018). Generally, previously published studies on this subject, only emphasize the diagnosis of the existing problem. On the other hand, few studies address how these pollutants, mainly heavy metals and metalloids, are mobilized from riverbed sediments and

transported through water (Courtin-Nomade et al., 2016; Dótor et al., 2014; Fawcett et al., 2015; Hiller et al., 2012).

Mexico is one of the countries affected by this problem since the mining activity extends throughout its territory, where environmental and human health hazards associated with mining have been detected (Espinosa and Armienta, 2007; Espinosa et al., 2009; Marmolejo-Rodríguez et al., 2011; Prieto García et al., 2016; Talavera Mendoza et al., 2016; Wurl et al., 2014). This study is focused on a mining district located within the limits of the Sierra de Huautla. Sierra de Huautla is also a biodiversity reserve with a semi-arid climate. Geographical and biological surveys of the area have already been undertaken (Garcia, 1981). Underground mines were abandoned without maintenance and tunnels flooded. Springs, with undefined recharge area or water from abandoned mines (flowing on tailing or flooded galleries) are used by the population as water supply for domestic and livestock needs, and then discharged into the rivers of the region. The highest concentrations of As, F, Fe, Mn, Pb and Cd were previously detected in various samples of ephemeral and perennial waters from runoff, old mine and groundwater (Esteller et al., 2015), thus exhibiting a sanitary risk for inhabitants of the town of Huautla due to these chemical pollutants in water, leading to use previously developed household removal systems of As (Avilés et al., 2013).

The toxicity of metals and metalloids (further named trace elements, TE), their fate and transport in the environment depend on their physicochemical forms, ie. their chemical speciation. Their ability to be mobilized also depends on their speciation. TE included in primary minerals, co-precipitated with secondary mineral phases or precipitated are not very mobile, whereas they are extremely mobile under dissolved species. Changes of pH and redox potential conditions (Borch et al., 2010; Davranche et al., 2003; Miao et al., 2006; Molina et al., 2013) related to rainfall and temperature, or the presence in the medium of dissolved organic or inorganic ligands (Buffle J., 1994; Pérez-Esteban et al., 2013; Yuan et al., 2007) may lead to a modification of their speciation and have consequences on their mobility (Huang, 2002; Sterckeman et al., 2000; Zhang and Zhang, 2010).

This study describes a detailed and comprehensive assessment of the TE contamination, including TE speciation, in waters (unfiltered water, dissolved and particulate phases) of different natures (surface waters, springs, groundwaters) and in sediments (granulometric fractions and

mineralogy). This investigation was performed in two sampling sites: the Huautla area, affected by past mining activities, and the Nexpa River unaffected by mining activities. The comparison of TE contents in the aforementioned sampling sites will contribute to the identification of the contamination source and to evaluate the level of TE enrichment according to the local geochemical baseline. Comparing TE contents in dissolved species and SPM in water, or in larger grains of sediment, this study will give new tools to evaluate TE mobility and reactivity, especially the role of soils, mines, sediments, and waters.

2. Geological and hydrological frameworks and weather conditions

2.1. Geological settings

The studied area is situated in Mexico, in the southern part of the Morelos state (18°26-18°32 N latitude and 98°58-99°10 W longitude), at the borders with Guerrero and Puebla states (Fig. 1, Table A, Supp. Info.). In the studied area, the basement consists of Paleozoic and Precambrian metamorphosed rocks. This basement is overlapped by a carbonaceous, sandy and silty platform (the Náhuatl terrane) deposited from lower to upper Cretaceous times (Ferrari et al., 2002; Ferrari L., 2007; Fitz-Díaz, 2001; Fries C., 1960; Fries C., 1966; Morán-Zenteno, 2007 ; Morán-Zenteno et al., 1999; Schaaf et al., 1995). During late Cenozoic times, the Laramide or 'Sierra Madre del Sur' orogeny folded the platform (Lugo Hubp, 1990; Martiny et al., 2000). In the southeastern part of the Huautla volcanic region, the volcanic rocks are represented by the altered Tamazola porphyry (Cerca et al., 2007) and volcanic materials from Oligocene to Miocene times (Alaniz-Álvarez et al., 2002; Blatter et al., 2001; Díaz-Bravo and Morán-Zenteno, 2011; González-Cervantes, 2007; González-Torres et al., 2013; Martiny et al., 2000; Morán-Zenteno et al., 2004; Rodrıguez-Licea, 1962; SECOFI, 1998). These lava-flows, dikes, volcanic tuffs units, and breccia, with intermediate to siliceous compositions, are described as the Huautla volcanic succession.

The village of Huautla and abandoned mining district host abundant hydrothermal alteration zones, epithermal veins related to a magmatic episode during the Paleocene time (González-Torres et al., 2013; Martiny et al., 2000). Metallic ore-deposits of Ag, Pb, Cu, and Au are distributed along

lineaments associated with haloes of hydrothermal alteration (Esteller et al., 2015; SGM, 2008). Descriptions of ore minerals indicate Fe-Ag-Cu-Pb-Zn-As sulfides associated with Cu and Pb-rich carbonates, quartz and iron oxides or metal-rich mineral in rocks and soils and further transported as metallic placer in river beds (Armienta et al., 2001; INEGI, 1983; SECOFI, 1998; SGM, 2008).

2.2. Weather and hydrography in the studied sites

In the Morelos state, annual precipitation average 1000 mm, with a wet period from June to September (around 200 mm per month) representing up to 80 % of the annual volume (CONAGUA database). Rainfall volumes average 60-70 mm in May or October and close to 10 mm for the other months. Nevertheless, the studied areas can also be affected by tropical storms producing flash floods, debris flows, particle transportation, or heat waves (such as in May to Nov. 2015). The average annual temperature ranges from 23 to 25 ºC with a mean maximum temperature of 40 °C. In the Sierra Huautla, altitude varies from 700 to 2400 m above sea level with a warm, dry and sub-humid climate. Temperatures vary from 7 to 27 °C during the year (meteorological stations: El Limón, Huautla, Jolalpa, Tepalcingo,(Garcia, 1981)) with total rainfall is about 900 to 1000 mm y^{-1} with maximum amounts of precipitation from July to September. In this mountain, drinking waters origin from scarce springs or shallow aquifer systems recharged by runoff through regolithic soil infiltration (INEGI, 1983).

The hydrology of the studied area consists of small watershed basins (0.3 to 3.2 km^2), as a part of the hydrological network (RH18) and tributaries of the Balsas River (Fig. A, Supp. Info.). The Nexpa River section, a part of the Cuautla larger basin, and the Huautla region with Quilamula River are both going into the Amacuzac River at the border of Guerrero and Puebla states. The Nexpa River has permanent water flow with irrigated plain or channelized allowing agriculture (Tilzapotla). Whereas, the Quilamula River and the other small tributaries in the Tilzapotla and Huautla regions are ephemeral and dry from November to April. Digital Elevation Model, produced SRTM (Shuttle Radar Topography Mission) Raster image (15 m resolution) and QGIS 2.18 software was completed with the georeferenced geological units, mining areas and fractures (SGM, 2008). Geomorphological analyzes (Wang and Liu, 2006) of the two areas of interest (Nexpa and Huautla), altitude varying from 700 to

1100 meter above sea level, show distinct topography and hydrological characteristics. Water produced in the Nexpa valley straight channels (km long) with low slopes (1 to 10 %) and sinuosity suitable for deposition of fine particles or remobilizing sediments. Whereas, Huautla district has steeper hill slopes (45 %) with potential more efficient transportation and erosion of the surrounding soils and volcanic plateaus.

3. Sampling and analytical methods

3.1. Sampling strategy and field measurements

A previous study (Esteller et al., 2015) was performed on 16 water samples (only the dissolved phase) from five flooded mines, three samples from dug wells and two samples from dams used as a source of drinking water by the inhabitants of the Huautla area. The highest concentrations of As and other toxic chemical elements (Fe, Mn, Pb, Cd) were detected in groundwater samples from flooded mines. For the present study, new samples were collected from the Huautla area as well as from the surrounding of the Cuautla-Nexpa River, to get a more complete picture of the local geochemical background. Specimens of water (in the unfiltrated waters, in the dissolved phases and in SPM) and sediments were gathered during two dry seasons, June 2013 and April 2016, and a wet season, September 2014.

Sediment specimens were sampled from three sampling sites at the banks of the Nexpa River (further referred to up, middle and down). Back to the lab, wet sediments were oven dried at 40 °C. A part of bulk sediments was then sieved (scarce grains above 630 μm) and weighed to perform granulometric separations.

In situ measurements were performed in waters: temperature, electrical conductivity (EC), pH, Oxydo Reduction Potential (ORP), dissolved dioxygen (DO), total dissolved solids (TDS), hardness, and turbidity. Water specimens were collected from all sampling sites. In the Nexpa River basin, they originated from groundwater from two springs (Manantial Cascabeles, Manantial Rio Nexpa) and from surface water from the Nexpa River (named up, middle and down). In the Huautla area, five groundwater samples were collected: from a spring (La Presita), two dug wells (shallow detrital

aquifer) used as drinking waters (Cruz Pintada, El Vivero) and two waters from abandoned and flooded mines (America and Pajaro Verde).

For each site, three water samples were collected: bulk waters (unfiltered water), dissolved phases (filtrate, <0.45 μm) and SPM (particle size >0.45 μm). Bulk waters contained both the dissolved phase and SPM. For dissolved phases, bulk waters were filtered with a syringe through a glass microfiber filters (GF/F grade 0.7 μm, preliminary burnt in an oven at 450 °C) installed into a polypropylene filter holder to collect: (1) dissolved phases for Dissolved Organic Carbon (DOC) and Dissolved Inorganic Carbon (DIC) analyses, (2) filters for Particulate Organic Carbon (POC) and Particulate Nitrogen (PN) measurements. Filter treatments, storage, and preservation were previously described (Lorrain et al., 2003). For major and trace element analyses, filtrations were also performed in a filtration unit (Nalgene, 1L) with acetate/nitrate cellulose filters (porosity 0.45 μm, Millipore, pre-cleaned in a 1% HNO_3 bath for 24 h, rinsed with Milli-Q water, dried and weighted). For each sampling date, a blank control was performed for the two filtration methods at the end of the day, consisting of filtration of MilliQ water performed after the usual cleaning procedure (performed between each sample). All wet filters were kept, dried under a laminar-flow in a class 100 clean laboratory, and weighted. The quantity of collected SPM was estimated in bulk waters on the field by turbidity measurements, and by calculation dividing the weight of deposited particles on filters by the filtrated water volume. Due to sampling troubles, these calculations were performed only for the first and last sampling (Jun. 2013 and Apr. 2016, dry periods) and only for waters originating from the Pajaro Verde mine in Sep. 2014 (the wet season). Bulk waters and filtrates were also collected and stored as previously described (Barats et al., 2014).

3.2. Granulometric, mineralogical and crystallographic analyses

Granulometric analyses and separations were performed for the first and second sampling. Laser particle-size analyzes of bulk sediments were performed with a Coulter LS200. The particle size distribution (2 mm to <0.3 μm) allowed the classification of sediments. Fine particles (< 2 μm, clay-size) were recovered by settling in deionized water. Particles coarser than 2 μm were recovered by sieving of 2-100 and 100-400 μm. In order to separate Fe-Mg-rich and Fe-Mg-poor minerals, grains

from the coarse-size fraction (100-400 μm) went through an isodynamic magnetic separation. Further, the mineralogy of the different size fractions was determined by X-ray diffraction and Scanning electron microscopy.

On bulk sediments, the occurrence of carbonates was determined on 3 g of sample by pressure calcimeter. The presence of carbonate in SPM collected on filters was also tested with HCl effervescence. The mineralogy of the different sediment fractions was examined: in coarse grains (100-400 μm) by optical and electron microscopes; and in fine grains (< 2 μm) by X-Ray Diffraction (XRD). Coarse grains were observed by transmitted light microscopy and grains mounted on carbon tape or epoxy mounted and polished. Mounted grains were observed by Scanning Electron Microscopy (SEM: EVO LS15 Zeiss) equipped with Energy Dispersive System (EDS: Oxford detector with a silicon drift detector) at the International Atomic Energy Agency in Monaco (electron beam 20 kV, 2.5 nA). SEM-EDS conduced to the qualitative chemistry of grain expressed as in weight (wt. %) and atomic (at. %) of major elements in samples. Crystallographic and mineral identification of sediments also was completed by XRD (Bruker-D5000 diffractometer; Cu $K_{\alpha 1+2}$, 40 kV, 25 mA equipped with a LynxEye detector 250 s/1° 2θ). X-ray diffractograms were conducted in random powder for 100 to 400 μm size fractions and oriented (air–dried, ethylene–glycol solvated, and heat–treated) preparations for fine fractions (< 2 μm) and suspended particulate matters (SPM > 0.45 μm).

3.3. Chemical analyses

For sediments (bulk, <2 μm, 100-400 μm) and particles (SPM > 0.45 μm), material was grinded and digested with 6 mL HNO_3 (Trace Metal Grade, 67 to 70% w/w, Fisher Chemical) and 2 mL HF (Ultra Trace Elemental Analysis 47-51% w/w, Optima, Fisher Chemical) in Teflon vessels in a closed microwave system (Ethos One, Milestone, 180°C, 30 min, 2000W). The mineralized solutions were then transferred to PE pre-cleaned tubes and gravimetrically diluted with Milli-Q water, up to a final volume of 50 mL. After proper additional dilution, these solutions were analyzed by Inductively Coupled Plasma Mass Spectrometry (ICP-MS Elan DRCII, Perkin Elmer).

For waters, major ions were analyzed by UV-spectrophotometry, volumetric measurements and atomic absorption spectrophotometer. Dissolved Organic Carbon (DOC) and Dissolved Inorganic

Carbon (DIC) were determined using TOC-V Analyser (Shimadzu®); Particulate Organic Carbon and Particulate Nitrogen (PN) using a Flash 2000 NC Soil Analyser (Thermo Scientific®). Trace elements (TE) were measured by Inductively Coupled Plasma Mass Spectrometry (ICPMS Elan DRCII, Perkin Elmer). Analytical procedures were previously described (Barats et al., 2014; Orani et al., 2018a; Orani et al., 2018b; Potot et al., 2012) and their validation in solid matrices was confirmed by repeated analyses of two certified reference materials, CRM, (MESS-2, estuarine sediment, and IAEA-158, marine sediment). Due to their low contents in CRM, Ag and Cd recoveries were not satisfactory. Pb measurements revealed also analytical troubles but only in the marine sediments (IAEA-158), perhaps related to the saline matrix, which is not the case in the further studied sediment (Table B, Supp. Info.). Speciation analyses were also performed for As in the dissolved phase of waters. An aliquot of Ethylene Diamine Tetra Acetic acid (EDTA) was added for the conservation of As species (100 µL EDTA at 0.125 mol L^{-1} into 15 ml of water sample), as previously recommended (Bednar et al., 2002). Analyses were performed by the hyphenated HPLC/ICP-MS method as previously described (Orani et al., 2018b).

3.4. Carbon ($\delta^{13}C_{DIC}$) and Sulfur ($\delta^{34}S_{SO4}$) stable isotopes in filtered waters

The $\delta^{13}C$ and $\delta^{34}S$ isotopic signatures of waters were measured in carbon and sulfur dissolved species (i.e. carbonates and sulfates, respectively) to underline processes related to the speciation of C and S. $BaCO_3$ precipitates were prepared on the field for $\delta^{13}C_{DIC}$ and $BaSO_4$ precipitates for $\delta^{34}S_{SO4}$ (Renac et al., 2009; Renac et al., 2020). These precipitates were realized with samples and blanks from each site to estimate contamination during sampling or transportation. $\delta^{13}C_{DIC}$ and $\delta^{34}S_{SO4}$ were measured on CO_2 and SO_2 obtained by Dumas combustion of $BaCO_3$ and $BaSO_4$ precipitates and analyzed by continuous flow analyses (Mass-spectrometry Elementar ISOPRIME 100 with Elemental analyzer VARIO, ISOLAB company). All $\delta^{13}C_{DIC}$ and $\delta^{34}S_{SO4}$ values are reported in per mil (‰) relative to international standards (V-SMOW and V-CDT). External error and reproducibility (2σ) for standards and replicates are ± 0.1 ‰ for $\delta^{13}C_{DIC}$, and ± 0.3 ‰ for $\delta^{34}S_{SO4}$.

3.5. Data treatment

Statistical data treatments were performed with XLSTAT (version 2014.05.5, Addinsoft, Paris, France) to realize correlation analyses.

In order to evaluate the sediment quality, three indices of contamination are used: Enrichment Factors (EF), Geo-accumulation Indexes (I_{geo}) and the Pollution Load Index (PLI), as already described elsewhere (Guan et al., 2016; Zahra et al., 2014). EF, I_{geo} and PLI calculations imply a normalization by the concentration in a background sample. In absence of analyses of fresh volcanic rocks and an incomplete bibliography regarding the TE compositions in the studied area, the upper continental crust (UCC) was defined as background sample with its chemical composition (Rudnick and Gao, 2014). EF calculations also need to define a reference element for normalization. Al, Ti, Fe, Mn, Rb are commonly used for their conservative proportion at neutral pH (Barbieri, 2016; Salati and Moore, 2010). Aluminum is usually chosen for its large abundance in crustal rocks and the no contamination concerns regarding pollution (Zhang et al., 2009). However, Al contents in bulk sediments were not measured. Consequently, Ti was used as the reference element for bulk sediments. For other solid samples, EF were calculated using Al as the reference element. The PLI estimation accounted for all TE (n=16) except Al and Ti. EF and Igeo are element-specific while PLI takes into account global contribution from all investigated pollutants. The total risk assessment for a metallic pollution will be evidenced by simultaneous: (1) EF > 5 revealing a significant enrichment of the targeted TE; (2) I_{geo} > 3 highlighting a strong contamination of the sediments by the targeted TE; and (3) a PLI > 1 demonstrating a global contamination (Barbieri, 2016).

The fine fraction of sediments is recognized to be the most reactive phase due to its high specific surface and usual high TE concentrations. Bulk sediments in the Nexpa River were composed mainly by coarse-size fractions (further measured in part IV.1.1.). In this study, sediments were assumed to be composed only by three fractions: fine, coarse-size Fe-Mg-rich and Fe-Mg-poor fractions. A least square method was used to evaluate the fraction responsible for the TE accumulation in the bulk sediments. The TE composition in sediments was hypothesized to result from TE concentrations of each fraction and their percentage of contribution (α, β, and γ) such as:

$$C_{\text{bulk sediment}} = \alpha \times C_{\text{fine fraction}} + \beta \times C_{\text{Fe-Mg-rich fraction}} + \gamma \times C_{\text{Fe-Mg-poor fraction}} \quad (1)$$

with the following condition: $\alpha + \beta + \gamma = 1$.

This equation was written for each TE (n = 16), except for Al and W, respectively, not measured and in low concentration in bulk sediments. The least square method was used to determine the three coefficients α, β, and γ. Due to the disparity of TE concentrations (especially high concentrations for Ti, Mn for example), these mathematical calculations were performed using normalization by the TE concentration in bulk sediments to give the same weight for the 16 equations:

$$1 = \alpha \times (C_{\text{fine fraction}}/C_{\text{bulk sediment}}) + \beta \times (C_{\text{Fe-Mg-rich fraction}}/C_{\text{bulk sediment}}) + \gamma \times (C_{\text{Fe-Mg-poor fraction}}/C_{\text{bulk sediment}}) \quad (2)$$

In order to identify major species in solution and to calculate saturation index with respect to minerals phases, PHREEQC software modeling was used with Lawrence Livermore National Laboratory thermochemical database (LLnL) (Parkhurst, 2013). In a second time, mineral phases in sediments and volcanic rocks were added to produce inverse models reflecting dissolution and precipitation associated with water-rock interactions from rainfall to spring, river and mine drainage.

4. Results

4.1. Sediments and SPM

4.1.1. Granulometry and mineralogy

Bulk sediments contained low contents of carbonate (0.14-0.21 %) with dominant coarse-size fractions (100-400 µm: 68 to 76 Weight %) and a minor fine-size fraction (< 2 µm: 0.3-1.8 Weight %). These riverine sediments were classified as fine to medium sand with poorly to moderate sortings (Fig. B, Supp. Info.). Among the coarse-size fraction, Fe-Mg-poor and Fe-Mg-rich- fractions represented around 80 Weight % and 20 Weight % respectively, i.e. 54-61 Weight % and 14-15 Weight % of the total sediment.

The mineralogy of the coarse-size fractions in sediments from the Nexpa River consisted of amphibole (hornblende) and iron oxide in the Fe-Mg-rich grains, and mainly fragmented andesine (a plagioclase feldspar) in the Fe-Mg-poor grains (Fig. C and D, Supp. Info). Some amphiboles presented preserved elongated shapes with shards of glass (Fig. C, Supp. Info., part B, C) and rare epidote grains. Some Fe-Mg-rich grains contained Ca-rich pyroxene and Fe oxide with magmatic textures

(Fig. C, Supp. Info., part D). The Fe-Mg-poor grains contained also small inclusions of Ca-pyroxene or Ca-rich hydroxyl phosphate (apatite) (Fig. 2, part A; Fig. C, part D, E, Supp. Info.). Grains of amphibole and feldspar showed alteration events with dissolution along cleavage (Fig. C, Supp. Info., part C) and polysynthetic macle (Fig. C, Supp. Info., part F). The two coarse-size fractions contained also traces of quartz.

The mineralogy of fine size fraction (< 2 μm) and SPM from waters (> 0.45 μm) from Nexpa and Huautla areas consisted of amorphous materials and clay minerals (Fig. 2, part C, D). In the Nexpa, the finest fractions contained amorphous material mixed with a dominant proportion of smectite, chlorite, biotite, quartz and a minor amount of feldspar. In the Huautla region, the fine particles contained a dominant proportion of a not well-crystallized phase (Cruz Pintada and El Vivero drinking waters) with kaolinite and smectite (America mine).

4.1.2. TE risk assessment in solid samples

TE concentrations measured in sediments from Nexpa River were presented in the Table 1. TE concentrations (As, Co, Cu, Mn, Pb, Zn) were found to be lower than those previously measured in surrounding rocks (Martiny et al., 2000), sediments collected in the Cuautla River (SECOFI, 1998), and the Sediment Quality Guidelines (SQG) (CCME; EPA, 2015; MacDonald et al., 2000), excepted for Mn concentrations in sediments of the Nexpa River. Enrichment factors (EF <5), Geo-Accumulation indices (I_{geo} <3) and Pollution Load Indices (PLI <1) (Table 2) demonstrated that sediments were not contaminated. Nevertheless, most TE had higher contents in Fe-Mg-rich fractions than in Fe-Mg-poor ones, except for Al, Ti, Sr, Li, and Cs. Fine fractions exhibited the highest concentrations of Al, Ti, Ba, Li, Cu, Rb, Cs, and similar As and Pb concentrations than in Fe-Mg-rich fractions. Statistical analysis were performed on average TE concentrations in sediments and their fractions to better constrain TE associations. The Pearson correlation matrix revealed two correlated groups (r^2> 0.9): the first one including Co, Mn, Sr, U and Zn, and a second one including As and Pb. It is worth noticing that Sr was anti-correlated with the other TE, agreeing with the Sr enrichment in the Fe-Mg-poor fractions.

Similar TE contents were found in SPM from riverine water and in fine fractions of sediments, with some exceptions (Table 1). A specific contamination related to Cd was demonstrated (EF = 192, I_{geo} = 7) (Table 2). This Cd contamination is not correlated to any other investigated TE. With a PLI < 1, a low environmental risk were demonstrated in the vicinity of the Nexpa River, except perhaps for Cd in SPM. SPM in waters originating from the Huautla area (springs, mines, and drinking waters) contained TE concentrations at least 10 times higher than all sampled sediments (for Ag, As, Cd, Li, Mo, W, and Zn) andriverine SPM in the Nexpa area (for Ag, As, Mo and Zn) (Table 1). The SQG, PLI >1, EF > 5 and I_{geo} > 3 of SPM confirmed the contamination of these solids (Table 2). This contamination is associated to As, Ag, Cd, and Zn in all SPM also, and occasionnally related to Mo and Mn in SPM from springs and drinking waters.

4.2. Waters

4.2.1. Field measurements (physicochemical parameters)

The physicochemical parameters indicated that all waters whatever the season are slightly basic (pH: 7.5-8.5), oxygenated (O_2: 1-2 mg L^{-1}) and oxidative (ORP: 100 to 400 mV) (Table C, Supp. Info.). Their electrical conductivity (EC) ranged from 240 to 3582 µS.cm^{-1}; water temperature and total alkalinity vary from 27 to 31 °C and 2 to 5 mmol L^{-1}, respectively. The highest EC values were measured during the dry and last sampling in Apr. 2016. Most of the physicochemical parameters measured in bulk waters respected the guidelines for water quality (WHO, 2017). The pH and O_2 (%) exceeded the WHO reference value for river waters, and EC only for spring waters from Cascabeles. High turbidities (> 5 NTU) and SPM contents (> 5 mg L^{-1}) were revealed in Nexpa River waters and in some drinking waters, exceeding the WHO regulation limit. Turbidity values (NTU) and estimated SPM contents (mg L^{-1}) revealed a significant linear relationship (r^2 = 0.98, n = 16).

4.2.2. Carbon and Nitrogen contents, and stable isotopes (C and S)

Dissolved inorganic carbon (DIC) concentrations ranged between 30 to 75 mg L^{-1}, with an average value of 51 ± 15 mg L^{-1} (Table D, Supp. Info.). Dissolved organic carbon (DOC) concentrations were lower than 6.5 mg L^{-1}, except in drinking waters (>12 mg.L^{-1}). Particulate Organic Carbon (POC) contents were usually low (< 0.2 to 6.31 mg L^{-1}). HCl acid tests onto SPM revealed the

absence of carbonates (particulate inorganic carbon) except from the filter originating from the Nexpa River downstream. Consequently, the total carbon contained in waters was supposed to be the sum of DIC, DOC, and POC. The dissolved inorganic carbon (DIC) represented the main portion of the total carbon (usually up to 80%) compared to total organic carbon (lower than 20 % for DOC + POC). In drinking waters, DIC contributions on total carbon were lower than on other waters (48-74%), exhibiting a high portion of DOC (23-43 %) and POC (3-10 %). DOC represented usually more than 80% of the organic carbon. But, POC contribution could reach 30-50 % of the organic carbon in drinking waters from "El Vivero" or in river waters (especially in the downstream part).

Particulate nitrogen (PN) revealed low content, except in drinking waters. These PN contents were not related to the amount of dissolved nitrogen (nitrate + nitrite), but significantly correlated to POC (PN = 0.137×POC, r^2 = 0.93, n= 16). This correlation may reveal that PN is mainly under organic matters, as particulate organic nitrogen.

The isotopic signature of carbon from DIC, $\delta^{13}C_{DIC}$, varied from -7.5 to -13.6 ‰ (Table D, Supp. Info.). River and drinking water indicated $\delta^{13}C_{DIC}$ values ranging from -11.2 and -13.7 ‰. The highest values were shown by waters from mines (Parajo Verde and America, with -7.9 and -10.5 ‰, respectively) and from the Cascabeles spring (-7.5 ‰). The $\delta^{13}C_{DIC}$ values were not correlated to the variations of DIC or total dissolved carbon (DIC+DOC). The isotopic signature of sulfur, $\delta^{34}S_{SO4}$, varied from 7.8 to 11 ‰. Like $\delta^{13}C_{DIC}$, river and drinking waters (around 8 ‰) had significant differences with waters from the Cascabeles spring and mines (around 10 ‰).

4.2.3. Major ions

The main ions contained in waters were Ca^{2+} (84 ± 66 mg L^{-1}) and HCO_3^- (222 ± 84 mg L^{-1}) or SO_4^{2-} (188 ± 277 mg L^{-1}) (Table D, Supp. Info.). Major ions contents in analyzed waters were significantly higher than the local rainwater composition and respected the WHO regulation, except for the Cascabeles sample. As previously shown with EC, waters from Cascabeles presented also high SO_4^{2-} and F^- concentrations, exceeding the WHO limits. As previously shown (Esteller et al., 2015), waters are usually calcium and carbonate-rich type (Fig. 3). Other waters exhibited a sodium-carbonate type such as for the America site (mines + surface draining), and a calcium-sulfate type such

as for the two springs named Cascabeles and Manantial Rio Nexpa, and surface waters (dry periods or downstream). During dry periods (June 2013 and April 2016), SO_4^{2-} concentrations in waters increased from the middle to lower part of the Nexpa River, until a change of the water nature from a calcium-carbonate to calcium-sulfate type. This change along the river runoff may be explained by water inputs of sulfate-rich waters, such as these two sulfate-rich springs.

4.2.4. TE risk assessment in waters

TE concentrations in bulk waters were presented in the Table 3. TE concentrations were lower than the WHO or Mexican limits, except for Al, As, and Mn. After filtration, Al, Pb, Mn, Zn and Cu concentrations measured in the dissolved phase of waters revealed significant lower contents, respecting quality regulations except for As and occasionally Mn in El Vivero drinking waters. This result agrees with the previous study which detected no contamination of Cd, Pb, and As in water samples (dissolved phase) collected in dug wells (Esteller et al., 2015). The study of TE proportions of dissolved species in waters revealed low dissolved contents of Al (17%), Pb (44%), Mn (52%), Zn (52%) and Cu (59%) (Table 4). These results demonstrate that SPM contain large amount of these TE. On the opposite, other TE occurred mainly under dissolved species: up to 70 % of the total content for Li, Ti, Co, Cd, Cs, and Ba and more than 90 % for As, Rb, Mo, Sr, Ag, W, and U. PHREEQC calculations indicated a main occurrence of TE under dissolved species in waters (cations, anions or complexes), except for Pb, Cu, and Mn as carbonates and Al, Zn and Ti as hydroxides (Table 3). This estimation confirmed the TE repartition between the dissolved phase and the particulate one, with higher Ti, Mn, Cu, Zn and Pb contents in SPM. This model reveals also second dominant species under sulfate forms, which is also in agreement with the sulfate-rich type of some waters.

Due to its environmental concern, a detailed study on As and its speciation was performed (Barats et al., 2016). Seasonal and inter-site variabilities of As concentrations in water were evaluated (Fig. 4), as previously perfomed in another hydrosystem (Barats et al., 2014). In the Nexpa River, As concentrations were close to 10 µg L^{-1}, with higher contents during dry periods (June 13 and April 16). During the dry periods, As concentrations increased from the upstream to the downstream river. Two springs, far away mining activities and with a sulfate water type, exhibited high As concentrations : 30 µg L^{-1} of As in Manantial Rio Nexpa, and 20 µg L^{-1} in Cascabelles. The increasing As and SO_4^{2-}

contents in river water noticed during the dry period may be related to decreasing runoff and an increasing lateral flow of the mentoned springs . In the Huautla region, potentially affected by mining activities, very high As contents were measured: ranging from 80 to 160 µg L^{-1} for waters from two mines, and from 44 to 51 µg L^{-1} for waters from a spring (La Presita) (Table 3). Similar high As contents were reported in waters from these two mines: 29-190 µg L^{-1} for Pajaro Verde mine ; 85-127 µg L^{-1} for America mine (Esteller et al., 2015). In drinking waters, As concentrations were lower than 10 µg L^{-1}, except in Cruz Pintada in June 2013 (12 µg L^{-1}). A seasonal variability seemed to occur with higher As concentrations during dry seasons, except in waters from springs and from the Pajaro Verde mine. Similar to the Nexpa river, this variability may be related to an increasing proportion of spring waters in the river while runoff decrease.

As speciation analyses performed by HPLC-ICPMS on the dissolved phases of waters revealed the unique occurrence of arsenate species. PHREEQC thermochemical calculations, lead with in-situ physicochemical conditions ($7 < pH < 9$ and $100\ mV < ORP < 400\ mV$), showed the occurrence of $HAsO_4^{2-}$ anions, which agrees with experimental measurements of the unique arsenate species.

5. Discussion

5.1. Origin of the TE occurrence in sediments

In order to unravel source of TE and their mobilty, the background mineralogy and TE enrichment in sediments was preliminary related to mineral phases coming from the surrounding rocks. Feldspars, pyroxenes, amphibole, volcanic glass observed in sediment, weathered volcanic rocks forming clays, oxides or transported grains such as carbonate, quartz from the upstream Cuautla region.

The chemical contribution of each sediment fraction (fine fraction: <2µm, Fe-Mg poor and rich fractions) to the global TE composition was evaluated by the least square method. The accuracy of the method was proved with the significant relationship between the estimated TE concentrations and measured concentrations (n= 16 elements, $r^2 = 0.9996$, $C_{estimated} = 0.8667\ C_{measured}$). The

proportions calculated by fitting eq. (2) turned out to be the following: α = 17.0 %, β = 41.7 % and γ = 41.3%, while their weight proportions were 0.3-1.8 Weight %, 14-15 Weight % and 54-61 Weight %, for the fine, Fe-Mg-rich, and Fe-Mg-poor fractions, respectively. The sum of Fe-Mg-rich and Fe-Mg-poor fractions represents the dominant reservoir of TE in sediments ($\beta + \gamma$ = 80%). The contribution of the fine and the coarse-size Fe-Mg-rich and Fe-Mg-poor fractions to the TE enrichment in sediments (calculated as the fraction: proportion of TE contribution % / Weight fraction proportion%) were at least 3 (=17/1.8), 9 (=41.7/15), 0.7 (=41.3/61) times higher than their occurrences. This result demonstrates that the fine and the coarse-size Fe-Mg-rich fractions are the main responsible of TE enrichments in the sediment.

The Fe-Mg rich fraction with pyroxene, amphibole, iron oxides and micas (Fig. 2 and C, Supp. Info.) are well known minerals with high Al, Fe, Mg, and Ti-contents (Deer, 2003) or other TE such as Co and Mn (pyroxene), and Zn (oxides) (Deer, 1997), in agreement with a statistical analysis revealing significant positive correlations between these TE. Fe-Mg-poor fractions contained dominant feldspar crystals (Fig. 2 and C, Supp. Info.), recognized to be enriched in Al, Sr, Rb (Deer, 2001), in agreement with significant negative correlations observed between Sr and the Co/Mn/Zn group. Fine fractions (< 2 μm) were demonstrated to contain clays and amorphous matters and to be TE rich. This TE enrichment may be supported by large specific surface of clays amorphous material combined with sorption processes (As) related to amorphous oxy-hydroxides of Zn, Mn, Al, Fe, As (Appelo, 2005; Christensen, 1984; Dzombak, 1990; Uddin, 2017). Sulfides were not observed in the different fractions of the sediment, but known to occur in local mines (exploited for Ag, Cu and Pb sulfides). They are also recognized to contain large amounts of As (Bowles J.F.W., 2011), which would argue with the significant positive correlation between As and Pb. These minerals probably occur under trace amounts, and may contribute to dissolved and particulate TE enrichment in sediments.

5.2. Origin of waters and their contamination

The majority of waters are of carbonate-rich type (Nexpa and Huautla) with dominant carbon species under DIC (ca. 45-83 mg L^{-1}), low TOC contents (< 18.3 mg L^{-1}) and negative $\delta^{13}C_{DIC}$ values

(from -13.9 to -7.9 ‰). This water chemical composition indicates either the dissolution of inorganic carbonates in sediments from the carbonaceous platforms located in the upstream Nexpa basin and not occurring in Huautla-Quilamula basin (Armienta et al., 2001; Esteller et al., 2015), or the mineralization of organic matter in soils. Except for drinking waters, DOC values in sampled waters are typical of rivers and lakes (Kalbitz et al., 2000; Thurman, 2012), suggesting that there is not organic contamination. The chemical composition of waters from the Nexpa River is suggested to be the local geochemical baseline, with a high background for As (around 10 µg L^{-1}). This water signature is suggested to derive from natural geochemical processes due to the water-rock interaction. Waters from the Nexpa River were demonstrated to contain also high SPM contents, which were not contaminated (PLI=1). The mineralogy of their SPM (amorphous + clays: dioctahedral smectite and Cd enriched) suggested that they are produced by weathering of volcanic rocks.

In this Mexican zone, the first trouble concerning the water contamination was demonstrated to be related to arsenic. This metalloid was found to occur in waters under dissolved species, as arsenate anions $HAsO_4^{2-}$, one of the most toxic species for humans (Cullen and Reimer, 1989; Hughes, 2002; Sakurai, 2002). As is supposed to originate either from desorption processes from clays, dissolution of oxi-hydroxides (Dzombak, 1990), or the oxidation of As-rich sulfides (Bowles J.F.W., 2011). In this study, As contaminations occurred in the dissolved phase of waters from springs and mines. The calcium-sulfate type of As-contaminated springs (Cascabeles and Manantial Rio Nexpa), far away from mining activities, argues with natural water-rock interactions related to the oxidation of sulfides in mineralized veins of the local geological formation, leading to sulfate- and As- rich waters. The other As contaminated waters (in the Huautla area) had a calcium-carbonate type, deriving from rainfall/volcanic rocks or sediment interactions. The As origin is probably related to mining activities due to the direct contact of recharge water with exploited minerals or operating mining residues. For these waters from flooded mines, the oxidation of sulfides were previously supposed to be the cause of As contaminations (Esteller et al., 2015). As sulfate and As in waters can present a potential common origin, the $\delta^{34}S_{SO4}$ values were determined. The $\delta^{34}S_{SO4}$ values of water from 7.8 to 11 ‰ confirm that dissolved sulfate do not derive from marine sulfate salts (gypsum or anhydrite; > +20 ‰; (Raab and

Spiro, 1991) but rather from continental sulfate minerals (+3 to +11 ‰; (Risacher et al., 2011). The geological context suggests that sulfates derived either from volcanic S (sulfate minerals such as gypsum, anhydrite found in the upstream Nexpa basin) or sulfides oxidation (galena or sphalerite of the mines). Even if no $\delta^{34}S$ values of sulfides are available in the literature for the Huautla region, the comparison of $\delta^{34}S_{SO4}$ (-7 to +3 ‰; (Dótor et al., 2014)) with $\delta^{34}S_{sulfide}$ values from Taxco mines (close to Huautla with similar volcanic context) (Camprubí et al., 2006), considered as analogous of the Huautla, suggest an abiotic oxidation of sulfides with higher $\delta^{34}S_{sulfide}$ values in Huautla than Taxco.

The second contamination trouble concerns drinking waters, threatened by both organic contamination and high SPM contents (Tables C and D, Supp. Info.). First, organic contamination were revealed by Total Organic Carbon contents (TOC= DOC+POC > 13 mg L^{-1}) above the European norm (2 mg L^{-1}), but mainly under DOC and in a lower extent under POC (30-50%). This organic contamination are suggested not to be related to anthropogenic activities (low-inhabitant density), but rather to autochthonous degradations of organic matters or adsorption of DOC in mineral soils (Ramanathan and Carmichael, 2008). Second, large amounts of SPM also threaten the quality of these drinking waters. These SPM contained amorphous materials and scarce clay minerals and they were enriched with TE (PLI > 3, Table 2). This TE enrichment in SPM is probably related to sorption processes onto clays (As) or the occurrence of amorphous TE-rich oxy-hydroxides (Appelo, 2005; Christensen, 1984; Dzombak, 1990; Uddin, 2017). The occurrence of TE-rich SPM threatens the water quality due to their high toxicity.

5. 3. Fate and dispersion of the contamination

Information concerning erosion and particle transportation in this sub-arid area are not available. However, the hydrological study of this Mexican zone performed with QGIS software revealed contrasted features. The low slopes (1 to 10 %) in the Nexpa area are suitable for deposition of fine particles or remobilizing sediments and on the opposite, steeper slopes (45 %) in the Huautla district facilitate the erosion of surrounding soils and water transportation. In this Huautla district, great attention has to be paid during wet periods when the erosion or water transportation may be

enhanced, because SPM from mines and springs were demonstrated to be highly contaminated by TE (enriched with Ag, As, Cd, and Zn, PLI > 3, Table 1 and 2). For the 3 sampling, these waters contained low amounts of SPM, but larger amounts of SPM may occur during wet periods and may conduce to the dissemination of these contaminated SPM in the downstream Quilamula River and to subsequent relevant sanitary troubles.

TE enrichment in sediments and in SPM from waters may be a second source of contamination because TE may be transferred from these solid phases to dissolved phases of waters. Fine fractions and SPM, enriched with TE, are very reactive to changes of physicochemical conditions (such as pH, Eh…). Their stability was tested by PHREEQC modeling to estimate their potential dissolution or precipitation. Minerals were selected based on their presence in sediments, local basement rocks (feldspars, pyroxenes, amphibole, volcanic glass, oxides, carbonate = aragonite, calcite, dolomite, magnesite, and quartz) and SPM (amorphous materials, kaolinite, smectite = saponite, nontronite; oxi-hydroxides = diaspore, anatase) (Fig. 2). Saturation indexes of water in equilibrium with these minerals revealed undersaturated water with respect to minerals such as andesite (feldspar, amphibole, pyroxene, sulfide), weathering or hydrothermal phases (kaolinite, saponite, nontronite), and in ore minerals (sulfide). These mineral phases (such as TE-rich sulfide and pyroxene) may thus contribute to TE transfers from the solid phase to the dissolved phase. Waters were also found oversaturated with respect to other minerals such as Al-Fe-rich smectite, illite-muscovite, kaolinite, dolomite, calcite, and Al oxy-hydroxides (gibbsite, boehmite, diaspore). On the opposite, these minerals (such as clays and oxi-hydroxides)may precipitate and and as a consequence, partially or totallly adsorb TE.

A hydrochemical thermodynamic modeling was used to estimate the transfer events (precipitation or dissolution) between water and minerals from sediments or rocks. The calculations used major elements composition of water (Table D, Supp. Info.), mineral phases previously identified (part 4.1.1.) and let free to dissolve or precipitate. Different waters were investigated: the upstream Nexpa River, drinking waters from Cruz Pintada or rainfall (Báez et al., 2006). In the Nexpa River, local water/rock interactions (from the upstream to downstream sampling sites) were demonstrated not

to occur, suggesting rather than the water chemical composition inherited from the upstream Nexpa basin.

Hydrochemical calculations were then performed to estimate the chemical composition of a water resulting from the interaction of rainfall and local minerals, compared to 2 local waters: Cruz Pintada drinking waters (As-poor, SPM-rich and sulfate-poor), La Presita spring waters (As-rich, SPM-poor, sulfate-poor). Three chemical and mineralogical conditions were applied: (a) the preferential dissolution of pyroxene compared to feldspar and clays in natural systems (all different type Ca-Mg-Fe pyroxenes must be under saturation); (b) Na-K feldspar can be in equilibrium, but Ca-feldspar must dissolve; (c) clays (Al-Fe smectite: Ca-or Na-saponite or nontronite) must precipitate or dissolved simultaneously. Among the thirteen solutions satisfying these three conditions, no solution involved the dissolution or precipitation of pyrite, which is in agreement with the neutral pH. Calculations suggest that source of sulfur in water are due to the dissolution of gypsum. These models indicate that Ca, Mg, Na, Si, P, F and Cl contents of waters derive from rainfall for Cl, the dissolution of gypsum, Na-Ca-feldspar, Ca-Mg pyroxene (Na, Ca, Si) and fluoroapatite (F, P), balanced by the precipitation of kaolinite and Ca-rich smectite (Si, Al, Ca, Na). The K-feldspar source of K is also undersaturated, but dissolved in smaller proportion compared to gibbsite and quartz (equal molar proportion). These calculations indicate that dissolution-oxidation of sulfides (ore minerals) aren't necessary to produce the water chemical composition of Cruz Pintada. The Cu-Pb-rich SPM in Cruz Pintada waters (SPM-rich and sulfate-poor) were interpreted as derived from the dissolution of carbonates. For La Presita spring (As-rich, SPM-poor, sulfate-poor), calculations indicate rather the potential dissolution of sulfides and the subsequent As-sorption/desorption processes onto oxyhydroxides or clays.

6. Conclusions

In this study, a local geochemical baseline of water quality was defined in this Mexican, which is of great interest for further environmental surveys. Water contaminations were demonstrated to be related either to the occurrence of dissolved As species, or to organic contamination and large amounts

of SPM enriched with TE in drinking waters. This study suggests three geochemical processes involved in the water contamination, none of them resulting directly from mining activity except for the case of water samples from flooded mines. The main identified processes were: 1/ oxidation of sulfides explaining the As contamination (natural or related to past mining activities) under dissolved species in water from springs and mines, 2/ natural degradation processes inducing organic contaminations in drinking waters, and 3/ natural processes of weathering and transport of TE-rich SPM due to the occurrence of clays and oxy-hydroxides. For waters from flooded mines, the As contamination is probably enhanced due to past mining activities. Finally, thermodynamic calculations demonstrate that transfer events could occur between minerals and waters: for example, the release of dissolved As from the dissolution of sulfides and subsequent As sorption/desorption processes onto oxyhydroxydes or clays, or Cu and Pb rich SPM in waters probably deriving from the dissolution of carbonates. This study thus confirms a significant human risk exposure to TE poisoning, and as well as a relevant sanitary hazard for inhabitants living in the Huautla district. This study give also new clues to reduce the sanitary risks: reducing suspended particles in waters or removing specific dissolved compounds.

7. Acknowledgments

This research was supported by the program ECOS/CONACYT/ANUIES for international cooperation between France and Mexico (project n°M12P01). The authors are grateful to M. Rozmaric and I. Levy and the Environment Laboratories of the International Atomic Energy Agency (IAEA in Monaco) for the access to electron microscopy facilities. The authors wish to thank B. Gonzales-Perez, A. Leclerc, H. Bali, S. El Hamaoui, students helping in water sampling and analyses; M. Bonnefoy for the last granulometric analyses and magnetic separations; to J.-P. Goudour for his do-it-yourself skills during apparatus crises.

8. References

Alaniz-Álvarez SA, Nieto-Samaniego AF, Morán-Zenteno DJ, Alba-Aldave L. Rhyolitic volcanism in extension zone associated with strike-slip tectonics in the Taxco region, southern Mexico. Journal of Volcanology and Geothermal Research 2002; 118: 1-14.

Appelo CAJ, Postma D. Geochemistry, groundwater and pollution. London: CRC Press, 2005.

Armienta MA, Villaseñor G, Rodriguez R, Ongley LK, Mango H. The role of arsenic-bearing rocks in groundwater pollution at Zimapán Valley, México. Environmental Geology 2001; 40: 571-581.

Avilés M, Garrido SE, Esteller MV, De La Paz JS, Najera C, Cortés J. Removal of groundwater arsenic using a household filter with iron spikes and stainless steel. Journal of environmental management 2013; 131: 103-109.

Báez AP, Belmont RD, García RM, Torres MCB, Padilla HG. Rainwater chemical composition at two sites in Central Mexico. Atmospheric Research 2006; 80: 67-85.

Barats A, Féraud G, Potot C, Philippini V, Travi Y, Durrieu G, et al. Naturally dissolved arsenic concentrations in the Alpine/Mediterranean Var River watershed (France). Science of The Total Environment 2014; 473-474: 422-436.

Barats A, Orani AM, Christophe R, Goudour J-P, Durrieu G, Saint-Martin H, et al. Behaviour and mobility of arsenic in a Mexican hydrosystem impacted by past mining activities. Arsenic Research and Global Sustainability: Proceedings of the Sixth International Congress on Arsenic in the Environment (As2016), June 19-23, 2016, Stockholm, Sweden - 2016.

Barbieri M. The importance of enrichment factor (EF) and geoaccumulation index (Igeo) to evaluate the soil contamination. J Geol Geophys 2016; 5: 2.

Bednar AJ, Garbarino JR, Ranville JF, Wildeman TR. Preserving the Distribution of Inorganic Arsenic Species in Groundwater and Acid Mine Drainage Samples. Environmental Science & Technology 2002; 36: 2213-2218.

Blatter DL, Carmichael ISE, Deino AL, Renne PR. Neogene volcanism at the front of the central Mexican volcanic belt: Basaltic andesites to dacites, with contemporaneous shoshonites and high-TiO2 lava. GSA Bulletin 2001; 113: 1324-1342.

Borch T, Kretzschmar R, Kappler A, Cappellen PV, Ginder-Vogel M, Voegelin A, et al. Biogeochemical Redox Processes and their Impact on Contaminant Dynamics. Environmental Science & Technology 2010; 44: 15-23.

Bowles J.F.W. HRAW, Vaughan D.J., Zussman J. Rock-forming minerals: non-silicates: oxides, hydroxides and sulphides. : Geological Society of London, 2011.

Brumbaugh WG, Tillitt DE, May TW, Javzan C, Komov VT. Environmental survey in the Tuul and Orkhon River basins of north-central Mongolia, 2010: metals and other elements in streambed sediment and floodplain soil. Environmental Monitoring and Assessment 2013; 185: 8991-9008.

Buffle J. DVRR. chapter "Uptake of trace metals by aquatic organisms". Chemical and biological regulation of aquatic systems. CRC Press, 1994.

Camprubí A, González-Partida E, Torres-Tafolla E. Fluid inclusion and stable isotope study of the Cobre–Babilonia polymetallic epithermal vein system, Taxco district, Guerrero, Mexico. Journal of Geochemical Exploration 2006; 89: 33-38.

CCME. Canadian Council of Ministers of the Environment, http://st-ts.ccme.ca/en/index.html?chems=4,8,9,12,15,16,20,21,61,63,62,65,71,123,124,127,129,131,138,139,197,198,200,211,213,225,226,229&chapters=3.

Cerca M, Ferrari L, López-Martínez M, Martiny B, Iriondo A. Late Cretaceous shortening and early Tertiary shearing in the central Sierra Madre del Sur, southern Mexico: Insights into the evolution of the Caribbean–North American plate interaction. Tectonics 2007; 26.

Christensen TH. Cadmium soil sorption at low concentrations: I. Effect of time, cadmium load, pH, and calcium. Water, Air, and Soil Pollution 1984; 21: 105-114.

CONAGUA database. Comission Nacional del Agua, http://sina.conagua.gob.mx/sina/tema.php?tema=precipitacion&n=estatal.

Courtin-Nomade A, Waltzing T, Evrard C, Soubrand M, Lenain J-F, Ducloux E, et al. Arsenic and lead mobility: From tailing materials to the aqueous compartment. Applied Geochemistry 2016; 64: 10-21.

Cullen WR, Reimer KJ. Arsenic speciation in the environment. Chemical Reviews 1989; 89: 713-764.

Davranche M, Bollinger J-C, Bril H. Effect of reductive conditions on metal mobility from wasteland solids: an example from the Mortagne-du-Nord site (France). Applied Geochemistry 2003; 18: 383-394.

de Souza ES, Texeira RA, da Costa HSC, Oliveira FJ, Melo LCA, do Carmo Freitas Faial K, et al. Assessment of risk to human health from simultaneous exposure to multiple contaminants in an artisanal gold mine in Serra Pelada, Pará, Brazil. Science of The Total Environment 2017; 576: 683-695.

Deer WA, Howie, R. A., Zussman, J. Rock-forming minerals: single-chain silicates. Vol 5B: UK Geological Society, 1997.

Deer WA, Howie, R. A., Zussman, J. Rock-forming minerals, sheet silicates: micas. Vol 3A: Geological Society of London, 2003.

Deer WA, Howie, R.A., Zussman, J. . Rock-Forming Minerals. Framework Silicates: Feldspars. Vol 4A. London: The Geological Society, 2001.

Díaz-Bravo BA, Morán-Zenteno DJ. The exhumed Eocene Sultepec-Goleta Volcanic Center of southern Mexico: record of partial collapse and ignimbritic volcanism fed by wide pyroclastic dike complexes. Bulletin of Volcanology 2011; 73: 917.

Dótor AA, Armienta-Hernández MA, Árcega-Cabrera F, Talavera-Mendoza O. Arsenic and metals transport processes in surface waters from the mining district of Taxco, Mexico: Stable isotopes application. [Procesos de transporte de arsénico y metales en aguas superficiales del distrito minero de Taxco, México: Aplicación de isótopos estables.] Hidrobiológica 2014; 24: 245-256.

Dzombak DA, Morel, F.M.M. Surface Complexation Modeling: Hydrous Ferric Oxide. New York: John Wiley & Sons,, 1990.

EPA. https://www.epa.gov/sites/production/files/2015-09/documents/r3_btag_fw_sediment_benchmarks_8-06.pdf. United States Environmental Protection Agency,, 2015.

Espinosa E, Armienta MA. Mobility and fractionation of Fe, Pb and Zn in river sediments from a silver and base-metals mining area: Taxco, México. Journal of Environmental Science and Health, Part A 2007; 42: 1391-1401.

Espinosa E, Armienta MA, Cruz O, Aguayo A, Ceniceros N. Geochemical distribution of arsenic, cadmium, lead and zinc in river sediments affected by tailings in Zimapán, a historical polymetalic mining zone of México. Environmental Geology 2009; 58: 1467-1477.

Esteller MV, Domínguez-Mariani E, Garrido SE, Avilés M. Groundwater pollution by arsenic and other toxic elements in an abandoned silver mine, Mexico. Environmental Earth Sciences 2015; 74: 2893-2906.

Fawcett SE, Jamieson HE, Nordstrom DK, McCleskey RB. Arsenic and antimony geochemistry of mine wastes, associated waters and sediments at the Giant Mine, Yellowknife, Northwest Territories, Canada. Applied Geochemistry 2015; 62: 3-17.

Ferrari L, López-Martínez M, Rosas-Elguera J. Ignimbrite flare-up and deformation in the southern Sierra Madre Occidental, western Mexico: Implications for the late subduction history of the Farallon plate. Tectonics 2002; 21: 17-1-17-24.

Ferrari L. V-MM, Bryan S. Magmatism and tectonics of the Sierra Madre Occidental and its relation with the evolution of western margin of North America, in Alaniz-Álvarez S.A., and Nieto-Samaniego, A.F., eds., Geology of México: Celebrating the Centenary of the Geological Society of Mexico: Geological Society of America Special Paper, . 422, 1-39, doi: 10.1130/2007.2422(01). 2007.

Fitz-Díaz E. Evolución estructural del sinclinorio de Zacango en el límite oriental de la Plataforma Guerrero-Morelos, [Undergraduate thesis]: México, Instituto Politécnico Nacional, 104 pp., 2001.

Fries C. J. Fries C., Jr., 1960, Geología del Estado de Morelos y de partes adyacentes de México y Guerrero, región central-meridional de México: Boletín Instituto de Geología, Universidad Nacional Autónoma de México. v. 60, 1960, pp. 236.

Fries C. J. Hoja Cuernavaca 14Q-h(8), Resumen de la geología de la Hoja Cuernavaca, Estado de Morelos: Instituto de Geología, Carta Geológica de México, Serie 1:100,000. Universidad Nacional Autónoma de México, 1966.

Garcia E. Modificaciones al Sistema de Clasificación Climática de Köppen para adaptarlo a las condiciones de la República Mexicana, 3a. ed. México: Offset Larios, 1981.

González-Cervantes N. Evolución del centro silícico de la Sierra de Nanchititla, Edo. de México y Michoacán, [M.Sc. thesis]: México, Universidad Nacional Autónoma de México,96 p., 2007.

González-Torres EA, Morán-Zenteno DJ, Mori L, Díaz-Bravo B, Martiny BM, Solé J. Geochronology and magmatic evolution of the Huautla volcanic field: last stages of the extinct Sierra Madre del Sur igneous province of southern Mexico. International Geology Review 2013; 55: 1145-1161.

Guan Q, Cai A, Wang F, Wang L, Wu T, Pan B, et al. Heavy metals in the riverbed surface sediment of the Yellow River, China. Environmental Science and Pollution Research 2016; 23: 24768-24780.

Hiller E, Lalinská B, Chovan M, Jurkovič Ľ, Klimko T, Jankulár M, et al. Arsenic and antimony contamination of waters, stream sediments and soils in the vicinity of abandoned antimony mines in the Western Carpathians, Slovakia. Applied Geochemistry 2012; 27: 598-614.

Huang PM, Bollag, J.-M., Denesi, N. Interactions between soil particules and microorganisms-Impact on the terrestrial ecosystem. : IUPAC Series on Analytical and Physical Chemistry of Environmental systems, 2002.

Hughes MF. Arsenic toxicity and potential mechanisms of action. Toxicology Letters 2002; 133: 1-16.

INEGI. Instituto Nacional de Estadisticas y Geografia, Geological map of Morelos state in Mexico (Cuernavaca). http://www.beta.inegi.org.mx/app/biblioteca/ficha.html?upc=702825279387, 1983.

Kalbitz K, Solinger S, Park J-H, Michalzik B, Matzner E. Controls on the dynamics of dissolved organic matter in soils: a review. Soil Science 2000; 165: 277-304.

Lorrain A, Savoye N, Chauvaud L, Paulet Y-M, Naulet N. Decarbonation and preservation method for the analysis of organic C and N contents and stable isotope ratios of low-carbonated suspended particulate material. Analytica Chimica Acta 2003; 491: 125-133.

Lugo Hubp J. Mapa geomorfológico del occidente de la cuenca de México. Investigaciones geográficas 1990: 01-19.

MacDonald DD, Dipinto LM, Field J, Ingersoll CG, Lvong ER, Swartz RC. Development and evaluation of consensus-based sediment effect concentrations for polychlorinated biphenyls. Environmental Toxicology and Chemistry 2000; 19: 1403-1413.

Marmolejo-Rodríguez AJ, Sánchez-Martínez MA, Romero-Guadarrama JA, Sánchez-González A, Magallanes-Ordóñez VR. Migration of As, Hg, Pb, and Zn in arroyo sediments from a semiarid coastal system influenced by the abandoned gold mining district at El Triunfo, Baja California Sur, Mexico. Journal of Environmental Monitoring 2011; 13: 2182-2189.

Martiny B, Martínez-Serrano RG, Morán-Zenteno DJ, Macías-Romo C, Ayuso RA. Stratigraphy, geochemistry and tectonic significance of the Oligocene magmatic rocks of western Oaxaca, southern Mexico. Tectonophysics 2000; 318: 71-98.

Miao S, DeLaune RD, Jugsujinda A. Influence of sediment redox conditions on release/solubility of metals and nutrients in a Louisiana Mississippi River deltaic plain freshwater lake. Science of The Total Environment 2006; 371: 334-343.

Molina RM, Schaider LA, Donaghey TC, Shine JP, Brain JD. Mineralogy affects geoavailability, bioaccessibility and bioavailability of zinc. Environmental Pollution 2013; 182: 217-224.

Morán-Zenteno DJ, Alba-Aldave LA, Solé J, Iriondo A. A major resurgent caldera in southern Mexico: the source of the late Eocene Tilzapotla ignimbrite. Journal of Volcanology and Geothermal Research 2004; 136: 97-119.

Morán-Zenteno DJ, Cerca, M., Keppie, J.D. The Cenozoic tectonic and magmatic evolution of southwestern México: Advances and problems of interpretation. In Geology of México: Celebrating the Centenary of the Geological Society of México, by Alaniz-Álvarez, S.A., and Nieto-Samaniego, Á.F. Geological Society of America Special Paper, 422, 71-91, doi: 10.1130/2007.2422(03). 2007.

Morán-Zenteno DJ, Tolson G, Martínez-Serrano RG, Martiny B, Schaaf P, Silva-Romo G, et al. Tertiary arc-magmatism of the Sierra Madre del Sur, Mexico, and its transition to the volcanic activity of the Trans-Mexican Volcanic Belt. Journal of South American Earth Sciences 1999; 12: 513-535.

Orani AM, Barats A, Vassileva E, Thomas OP. Marine sponges as a powerful tool for trace elements biomonitoring studies in coastal environment. Marine Pollution Bulletin 2018a; 131, Part A: 633-645.

Orani AM, Barats A, Zitte W, Morrow C, Thomas OP. Comparative study on the bioaccumulation and biotransformation of arsenic by some northeastern Atlantic and northwestern Mediterranean sponges. Chemosphere 2018b; 201: 826-839.

Parkhurst DL, Appelo, C.A.J. . Description of input and examples for PHREEQC version 3-A computer program for speciation, batch-reaction, one-dimensional transport, and inverse geochemical calculations, U.S. Geological Survey Techniques and Methods, book 6, chap. A43, 497 p., available only at https://pubs.usgs.gov/tm/06/a43/. 2013.

Parviainen A, Marchesi C, Suárez-Grau JM, Garrido CJ, Pérez-López R, Nieto JM, et al. Unraveling the impact of chronic exposure to metal pollution through human gallstones. Science of The Total Environment 2018; 624: 1031-1040.

Pérez-Esteban J, Escolástico C, Moliner A, Masaguer A. Chemical speciation and mobilization of copper and zinc in naturally contaminated mine soils with citric and tartaric acids. Chemosphere 2013; 90: 276-283.

Potot C, Féraud G, Schärer U, Barats A, Durrieu G, Le Poupon C, et al. Groundwater and river baseline quality using major, trace elements, organic carbon and Sr-Pb-O isotopes in a Mediterranean catchment: The case of the Lower Var Valley (south-eastern France). Journal of Hydrology 2012; 472-473: 126-147.

Prieto García F, Acevedo Sandoval OA, Pérez Moreno F, Prieto Méndez J, Canales Flores RA. Arsenic contamination in groundwater in Zimapan, Hidalgo, Mexico. Desalination and Water Treatment 2016; 57: 13038-13047.

Raab M, Spiro B. Sulfur isotopic variations during seawater evaporation with fractional crystallization. Chemical Geology: Isotope Geoscience section 1991; 86: 323-333.

Ramanathan V, Carmichael G. Global and regional climate changes due to black carbon. Nature Geoscience 2008; 1: 221.

Renac C, Gal F, Ménot RP, Squarcioni P, Perrache C. Mean recharge times and chemical modelling transfers from shallow groundwater to mineralized thermal waters at Montrond-les-Bains, Eastern Massif Central, France. Journal of Hydrology 2009; 376: 1-15.

Renac C, Moine B, Goudour J-P, LeRomancer M, Perrache C. Stable isotope study of rainfall, river drainage and hot springs of the kerguelen archipelago, SW Indian Ocean. Geothermics 2020; 83: 101726.

Risacher F, Fritz B, Hauser A. Origin of components in Chilean thermal waters. Journal of South American Earth Sciences 2011; 31: 153-170.

Rodrıguez-Licea F, Sanchez-Montes de Oca, R., Gamboa-Avitia, A. Estudio geologico - minero del Distrito de Huautla, Morelos. Archivo Tecnico del Consejo de Recursos Minerales. Servicio Geologico Mexicano, Mexico., 1962.

Rudnick RL, Gao S. 4.1 - Composition of the Continental Crust A2 - Holland, Heinrich D. In: Turekian KK, editor. Treatise on Geochemistry (Second Edition). Elsevier, Oxford, 2014, pp. 1-51.

Sakurai T. Review: Biological effects of organic arsenic compounds in seafood. Applied Organometallic Chemistry 2002; 16: 401-405.

Salati S, Moore F. Assessment of heavy metal concentration in the Khoshk River water and sediment, Shiraz, Southwest Iran. Environmental Monitoring and Assessment 2010; 164: 677-689.

Schaaf P, Morán-Zenteno D, Hernández-Bernal MdS, Solís-Pichardo G, Tolson G, Köhler H. Paleogene continental margin truncation in southwestern Mexico: Geochronological evidence. Tectonics 1995; 14: 1339-1350.

SECOFI. Informe de la carta geologica-minera y geoquimica. Hoja de Cuernavaca E14-5. Secretarıa de Comercio y Fomento Industrial. Secretarıa de Comercio y Fomento Industrial, Consejo de Recursos Minerales- Coordinacion general de Mineria, Chilpancingo, Mexico., 1998.

SGM. Monografia geologico-minera del Estado de Morelos Servicio Geologico Minero, Secretaria de Economia, Gobierno Federal, Mexico, 2008.

Sterckeman T, Douay F, Proix N, Fourrier H. Vertical distribution of Cd, Pb and Zn in soils near smelters in the North of France. Environmental Pollution 2000; 107: 377-389.

Talavera Mendoza O, Ruiz J, Díaz Villaseñor E, Ramírez Guzmán A, Cortés A, Salgado Souto SA, et al. Water-rock-tailings interactions and sources of sulfur and metals in the subtropical mining region of Taxco, Guerrero (southern Mexico): A multi-isotopic approach. Applied Geochemistry 2016; 66: 73-81.

Thurman EM. Organic geochemistry of natural waters: Springer Netherlands, 2012.

Uddin MK. A review on the adsorption of heavy metals by clay minerals, with special focus on the past decade. Chemical Engineering Journal 2017; 308: 438-462.

Wang L, Liu H. An efficient method for identifying and filling surface depressions in digital elevation models for hydrologic analysis and modelling. International Journal of Geographical Information Science 2006; 20: 193-213.

Wurl J, Mendez-Rodriguez L, Acosta-Vargas B. Arsenic content in groundwater from the southern part of the San Antonio-El Triunfo mining district, Baja California Sur, Mexico. Journal of Hydrology 2014; 518: 447-459.

Yuan S, Xi Z, Jiang Y, Wan J, Wu C, Zheng Z, et al. Desorption of copper and cadmium from soils enhanced by organic acids. Chemosphere 2007; 68: 1289-1297.

Zahra A, Hashmi MZ, Malik RN, Ahmed Z. Enrichment and geo-accumulation of heavy metals and risk assessment of sediments of the Kurang Nallah—Feeding tributary of the Rawal Lake Reservoir, Pakistan. Science of The Total Environment 2014; 470-471: 925-933.

Zhang M, Zhang H. Co-transport of dissolved organic matter and heavy metals in soils induced by excessive phosphorus applications. Journal of Environmental Sciences 2010; 22: 598-606.

Zhang W, Feng H, Chang J, Qu J, Xie H, Yu L. Heavy metal contamination in surface sediments of Yangtze River intertidal zone: An assessment from different indexes. Environmental Pollution 2009; 157: 1533-1543.

Zhang Z, Lu Y, Li H, Tu Y, Liu B, Yang Z. Assessment of heavy metal contamination, distribution and source identification in the sediments from the Zijiang River, China. Science of The Total Environment 2018; 645: 235-243.

Declaration of interests

☒ The authors declare that they have no known competing financial interests or personal relationships that could have appeared to influence the work reported in this paper.

☐The authors declare the following financial interests/personal relationships which may be considered as potential competing interests:

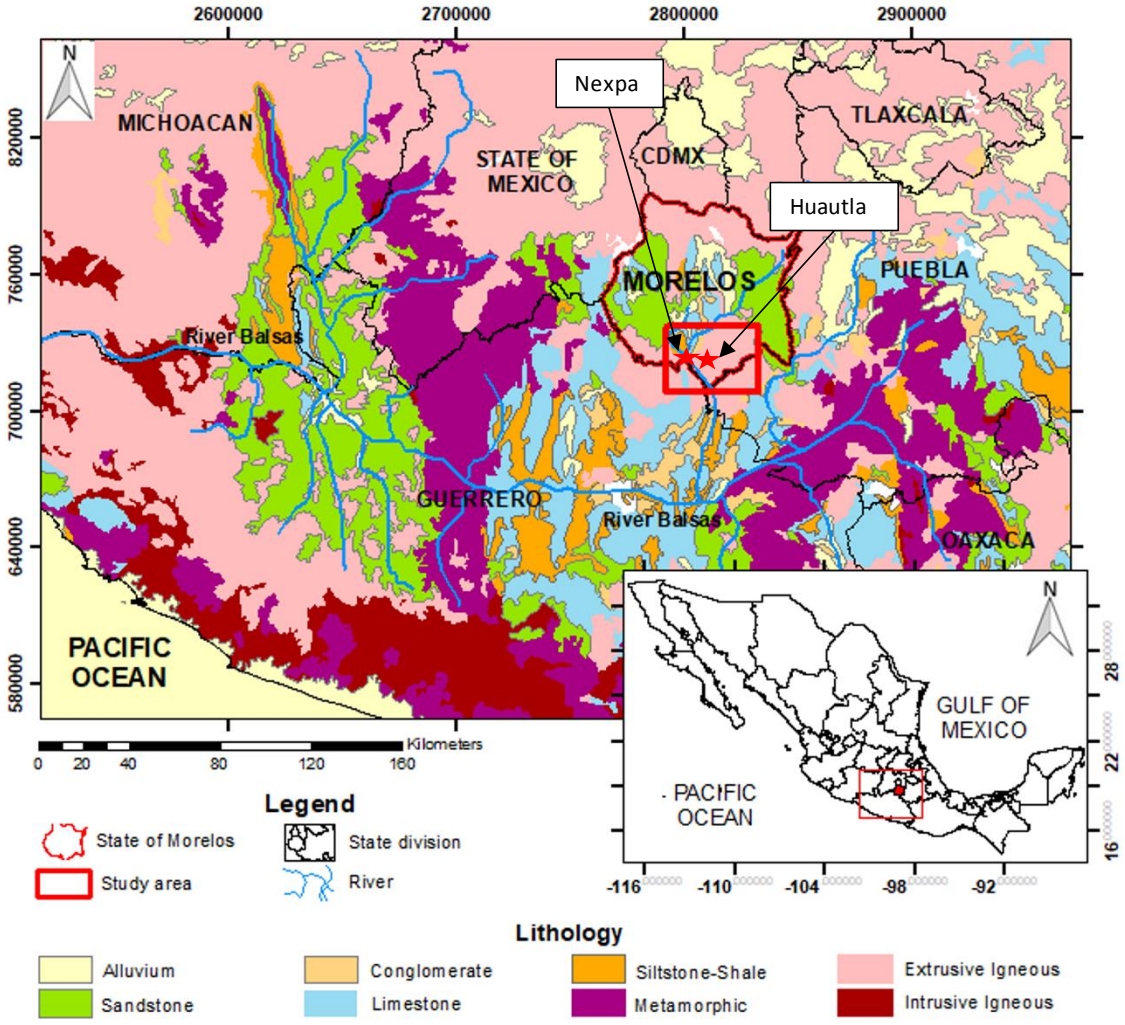

Figure 1 : Map of the sampling area in the Morelos state (Sierra Huautla, Mexico) with the simplified geological features (SECOFI, 1998; SGM, 2008) and the large watershed basin of the Rio Balsas.

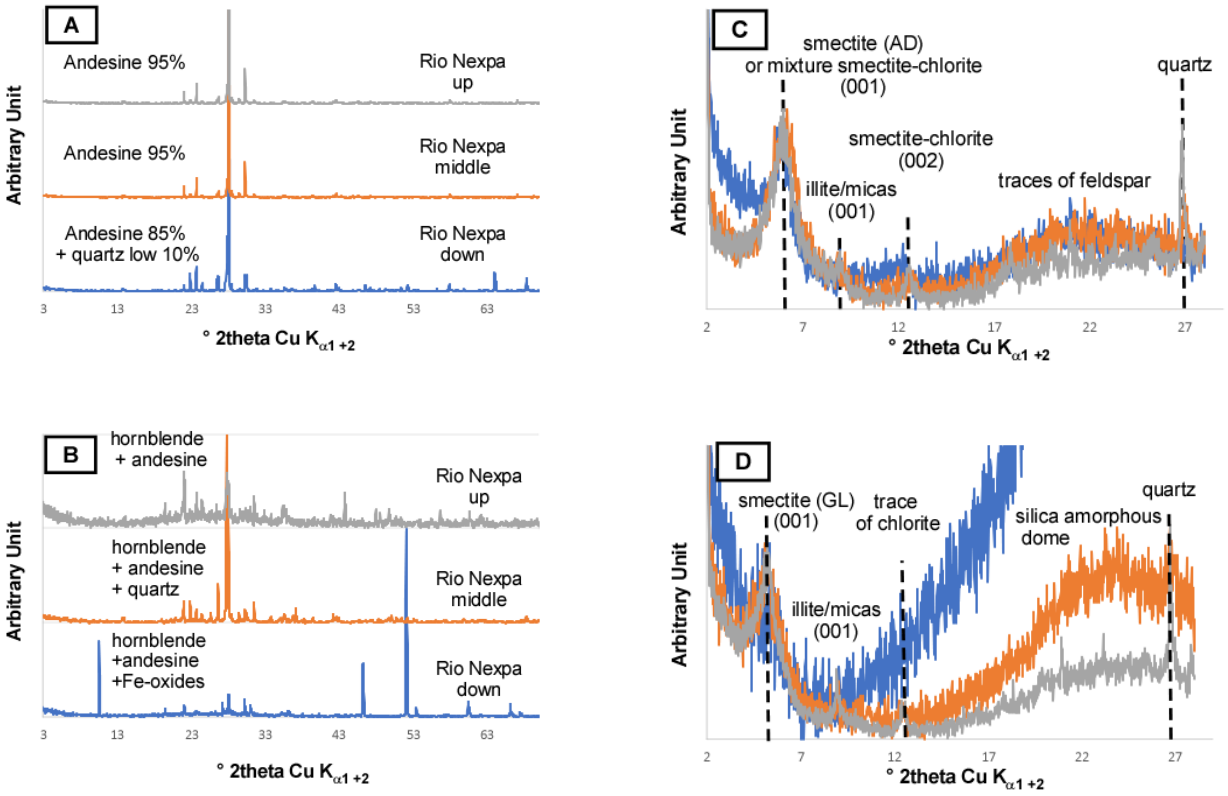

Figure 2 : X-ray diffractograms of different fractions of sediments from the Nexpa River of the first sampling: A) the coarse size Fe-Mg-poor fraction, B) the coarse size Fe-Mg-rich fraction, and the fine size fraction (< 2 μm) C) air-dried oriented preparation and D) glycolated oriented preparation to evaluate the amount of swelling clays (smectite).

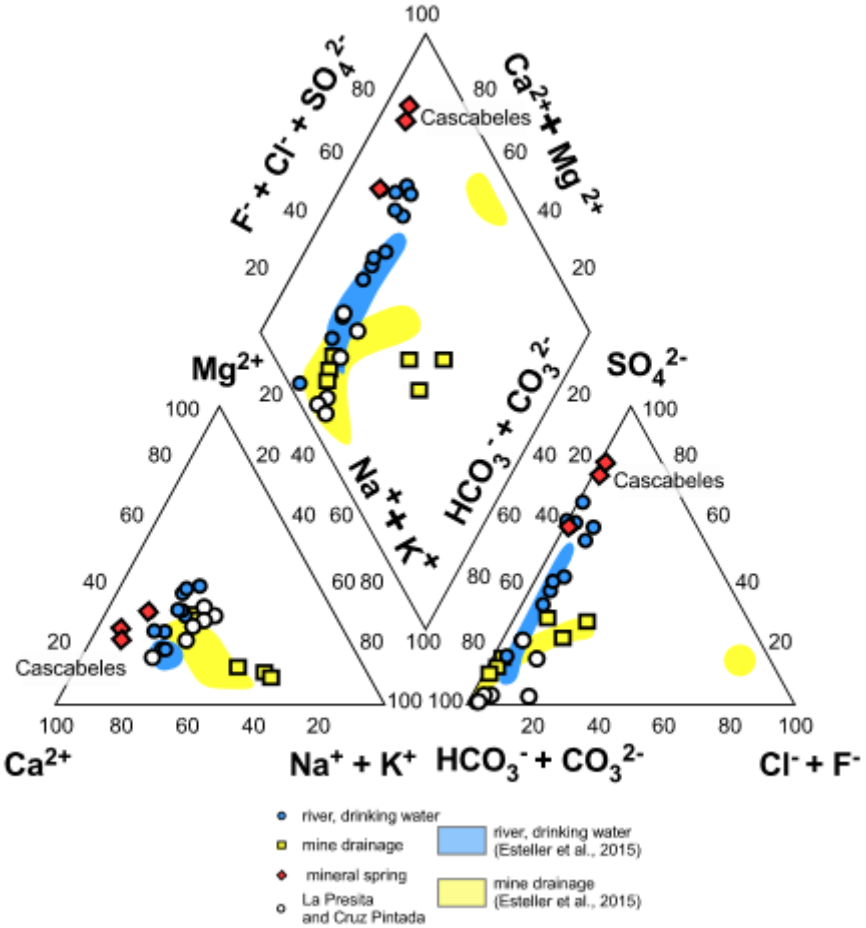

Figure 3 : Piper diagram comparing the composition of major ions concentrations in the dissolved phase of different waters.

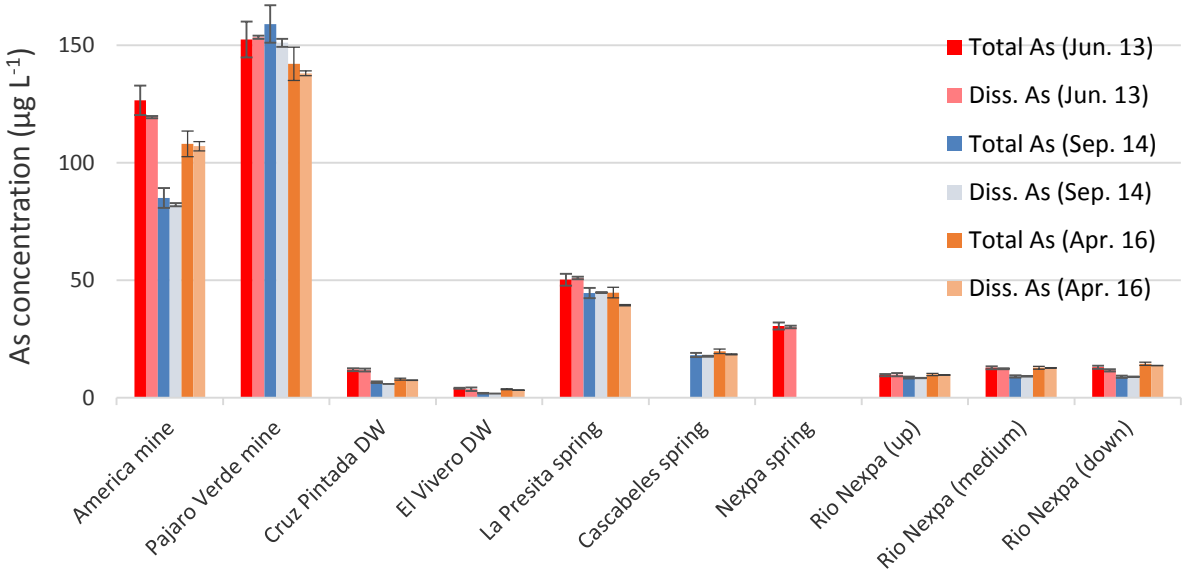

Figure 4 : Variations of As concentrations in bulk waters (total As) and in filtered waters (dissolved As) according to sampling sites and sampling dates. The bar lines show the standard deviation on analytical measurements (n = 3). The initial DW represent drinking waters.

Table 1 : Average chemical composition of sediments, their fractions, and Suspended Particulate Matters (SPM) collected in this study compared to Upper Continental Crust ([a]Rudnick et al., 2014), local rocks ([b]Martiny et al., 2000) and sediments from the East of Huautla district ([c]SECOFI, 1998), and freswater Sediment Quality Guidelines (SQG) from [d] U.S. Environmental Protection Agency EPA or [e] the Canadian Council of Ministers of the Environment. For the data measured in the present study, the expanded uncertainty (k=2) was estimated as 10%.

		Bulk sediments	Fine fractions of sediments	Fe-Mg-rich fractions	Fe-Mg-poor fractions	SPM from river	SPM from springs	SPM from drinking waters	SPM from mines	Upper Continental Crust[a]	Local rocks and sediments	Sediment Quality Guidelines
	n	9	6	6	6	6	4	4	5			
Concentrations (mg kg^{-1})	Al	-	89386	51167	82000	96731	27471	46230	25876	81500	66125[b]	-
	Ti	4454	5243	3173	3988	3317	1786	978	958	3836	5700[b]	-
	Mn	627	631	836	102	574	200	11685	1049	774	950[b]/ 561[c]	460[d]
	Rb	20.3	27.2	16.6	9.43	39.7	27.0	21.8	27.8	84	42.8[b]	-
	Co	18.9	20.0	29.3	3.23	7.31	8.52	7.67	2.68	17.3	-	50[d]
	Cu	15.4	41.2	25.0	8.70	15.5	31.1	20.9	56.3	28	29[b]	31.6[d]/35.7[e]
	Cs	1.23	3.16	0.432	0.503	2.72	3.81	2.15	2.56	4.9	-	-
	W	0.036	0.432	0.651	0.414	0.580	1.16	0.389	1.26	1.9	-	-
	U	1.02	1.06	1.25	0.490	0.597	2.08	2.03	1.08	2.7	-	-
	Sr	338	280	209	452	505	1429	254	360	320	426[b]	-
	Ba	225	527	203	177	202	92	4395	161	628	389[b]	-
	Pb	5.00	7.68	7.60	4.26	6.54	9.98	4.54	88	17	54.4[c]	35.8[d]/35[e]
	Zn	87	109	131	23	106	13243	2658	5458	67	-	121[d]/123[e]
	Li	19.2	41.3	11.6	18.9	46.4	183	160	74.0	24	-	-
	Mo	1.10	0.856	1.65	0.722	1.11	12.1	10.4	5.1	1.1	-	--
	As	4.49	5.43	5.67	3.68	5.23	67.8	45.8	69.9	4.8	12.5[c]	9.8[d]/5.9[e]
	Cd	<0.5	<0.5	<0.5	<0.5	20.5	110	30.4	18.9	0.09	0.8[c]	0.99[d]/0.6[e]
	Ag	<0.5	<0.5	<0.5	<0.5	<0.5	11.3	6.83	45.0	0.053	-	1[d]

Table 2 : Assessment of pollution level in sediments, their fractions, and Suspended Particulate Matters (SPM) estimating Enrichment Factors (EF), Geo-Accumulation Index (I_{geo}), Pollution Load Index (PLI).

		Bulk sediments	Fine fractions of sed.	Paramagnetic fractions of sed.	Diamagnatic fractions of sed.	SPM from river	SPM from springs	SPM from drinking waters	SPM from mines
Enrichment factors (EF)	Mn	1	1	2	0	1	1	**27**	4
	Zn	1	1	3	0	1	**586**	**70**	**257**
	Ba	0	1	1	0	0	0	**12**	1
	Sr	1	1	1	1	1	**13**	1	4
	Li	1	2	1	1	2	**23**	**12**	**10**
	Co	1	1	3	0	0	1	1	0
	Cu	0	1	1	0	0	3	1	**6**
	As	1	1	2	1	1	**42**	**17**	**46**
	Rb	0	0	0	0	0	1	0	1
	Cd	-	-	-	-	**192**	**3622**	**595**	**663**
	Pb	0	0	1	0	0	2	0	**16**
	Ag	-	-	-	-	-	**633**	**227**	**2675**
	Mo	1	1	2	1	1	**33**	**17**	**15**
	Cs	0	1	0	0	0	2	1	2
	W	0	0	1	0	0	2	0	2
	U	0	0	1	0	0	2	1	1
Geo-Accumulation indices (I_{geo})	Mn	-1	-1	0	-4	-1	-3	**3**	0
	Zn	0	0	0	-2	0	**7**	**5**	**6**
	Ba	-2	-1	-2	-2	-2	-3	2	-3
	Sr	-1	-1	-1	0	0	2	-1	0
	Li	-1	0	-2	-1	0	2	2	1
	Co	0	0	0	-3	-2	-2	-2	-3
	Cu	-1	0	-1	-2	-1	0	-1	0
	As	-1	0	0	-1	0	**3**	**3**	**3**
	Rb	-3	-2	-3	-4	-2	-2	-3	-2
	Cd	-	-	-	-	**7**	**10**	**8**	**7**
	Pb	-2	-2	-2	-3	-2	-1	-2	2
	Ag	-	-	-	-	-	**7**	**6**	**9**
	Mo	-1	-1	0	-1	-1	**3**	**3**	I
	Cs	-3	-1	-4	-4	-1	-1	-2	-2
	W	-6	-3	-2	-3	-2	-1	-3	-1
	U	-2	-2	-2	-3	-3	-1	-1	-2
PLI	-	0.7	1.1	0.9	0.5	1.1	**3.4**	**3.2**	**3.1**

Table 3 : Trace element concentrations in bulk waters (µg L^{-1}) compared to the local rainwater (at Cuernavaca City ; Garrido et al., 2017), the Mexican Standard (NOM-127-SSA1-1994) and World Health Organization (WHO) limits. The symbol S1, S2 and S3 stand for the first, second and third sampling. All TE value above the WHO limits were underlined. For the data measured in the present study, the expanded uncertainty (k=2) was estimated as 5%.

Concentrations in bulk waters (µg L^{-1})	Nature	Li	Al	Ti	Mn	Co	Cu	Zn	As	Rb	Sr	Mo	Ag	Cd	Cs	W	Ba	Pb	U
America S1	Waters draining mines	233	64.0	6.92	52.4	0.385	0.938	19.8	127	5.69	928	7.29	<0.007	0.062	1.04	0.124	29.9	6.83	3.84
America S2		175	180	6.80	72.5	0.457	4.09	28.6	85	4.52	1170	3.17	0.030	0.077	0.874	0.499	98.3	3.17	4.48
America S3		233	24.9	7.17	36.5	0.227	1.45	6.87	108	5.72	851	8.13	0.045	0.061	1.54	0.178	27.0	1.03	5.39
Pajaro Verde S1		38.7	1.42	8.08	0.674	0.105	<0.03	1.61	152	3.38	429	0.064	<0.007	0.089	1.93	0.086	13.6	0.189	0.981
Pajaro Verde S2		33.9	<0.8	7.57	3.15	0.136	5.77	72.7	151	3.34	451	0.127	0.014	0.153	2.00	0.107	389	0.856	0.986
Pajaro Verde S3		38.56	12.3	18.0	1.60	0.458	1.70	38.2	138	3.49	436	0.568	0.057	0.166	1.97	0.378	15.0	0.471	0.857
Cruz Pintada S1	Drinking water	4.83	25.7	5.89	130	0.214	<0.03	5.49	11.9	5.41	447	0.493	<0.007	<0.005	0.043	0.079	153	0.221	1.55
Cruz Pintada S2		3.23	492	12.5	162	0.835	5.89	49.7	6.55	3.06	220	0.249	0.020	0.028	0.078	1.34	872	0.599	0.274
Cruz Pintada S3		4.09	22.7	8.33	369	0.260	1.21	8.58	7.87	5.08	467	0.404	0.044	0.021	0.059	0.129	140	0.486	0.324
El Vivero S1		0.52	28.3	6.03	504	0.528	0.768	6.74	3.95	3.03	402	0.399	<0.007	0.001	0.017	0.007	98.5	0.660	0.370
El Vivero S2		1.22	155	5.67	145	0.353	14.6	56.3	1.84	1.34	190	0.194	<0.007	0.007	0.027	1.01	93.2	0.840	0.152
El Vivero S3		0.265	844	19.2	439	0.632	9.07	250	3.56	2.93	386	0.625	0.039	0.021	0.108	0.086	386	2.36	0.827
La Presita S1	Springs	79.1	5.40	10.1	0.599	0.167	0.444	17.6	50.2	4.35	495	0.106	<0.007	0.008	1.64	0.048	4.29	0.523	2.54
La Presita S2		65.0	<0.8	8.96	1.50	0.148	4.50	34.5	44.7	3.71	592	0.116	0.021	0.033	1.58	1.48	170	0.081	3.85
La Presita S3		49.8	5.35	14.5	0.266	0.172	0.863	17.8	44.7	3.85	550	0.19	0.032	<0.005	1.41	0.107	3.39	0.323	2.41
Cascabeles S2		48.6	<0.8	7.42	2.33	0.670	5.71	22.3	18.1	6.85	3840	5.13	0.013	0.051	1.86	0.563	67.1	0.070	1.36
Cascabeles S3		39.2	5.63	15.4	0.265	1.19	0.667	6.51	19.7	7.94	3850	6.80	0.051	0.066	2.03	0.159	19.0	0.335	1.41
Manantial Rio Nexpa S1		45.0	1.75	6.78	0.239	0.310	<0.03	15.1	30.4	6.04	1803	14.8	<0.007	0.061	1.40	0.042	23.3	0.021	1.95
Rio Nexpa up S1	Riverwater	29.8	935	29.4	87.2	1.50	2.50	44.6	9.57	11.8	1069	1.22	<0.007	0.071	0.067	0.030	156	1.85	2.75
Rio Nexpa up S2		32.1	<0.8	30.1	44.1	0.745	5.27	7.28	8.50	10.5	1020	1.16	0.012	0.018	0.207	0.844	94.3	0.215	2.80
Rio Nexpa up S3		18.0	64	15.3	4.97	0.622	2.26	5.38	9.63	14.4	1253	2.33	0.050	0.072	0.215	0.136	89.5	0.397	3.89

Rio Nexpa middle S1		30.0	600	28.2	58.5	1.26	1.37	10.7	12.7	12.0	1302	2.03	<0.007	0.024	0.136	0.037	130	1.04	3.17
Rio Nexpa middle S2		34.0	<0.8	36.2	47.7	0.978	5.29	14.4	8.99	10.2	1100	1.41	0.016	0.028	0.183	0.023	165	0.537	2.79
Rio Nexpa middle S3		18.4	352	17.7	11.7	0.745	2.14	5.22	12.7	13.6	1408	3.69	0.062	0.088	0.359	0.123	80.8	0.491	3.38
Rio Nexpa down S1		32.9	2219	37.5	193	2.51	3.77	21.6	12.9	13.2	1331	1.44	<0.007	0.072	0.140	0.017	177	2.67	3.25
Rio Nexpa down S2		34.3	<0.8	32.0	41.8	0.734	5.36	47	8.90	10.2	1100	1.35	0.014	0.025	0.159	0.023	486	0.127	2.80
Rio Nexpa down S3		20.9	545	27.8	14.8	0.891	3.09	10.2	14.4	13.7	1413	3.27	0.064	0.088	0.266	0.128	85.3	0.539	3.43
WHO[a]/Mexican[b] limits		-	200 [a,b]	-	500/150	-	2000 [a,b]	3000/5000	10/25	-	-	70 [a]	-	3/5	-	-	1300/700	10 [a,b]	30 [a]
Dominant species (PHREEQC)		Li^+	$AlO(OH)_2(s)$ $Al(OH)_3(s)$	$Ti(OH)_{4(s)}$	$MnCO_{3(s)}$	$HCoO_2^-$	$CuCO_3(s)$	$Zn(OH)_{2(s)}$	$HAsO_4^{2-}$	Rb^+	Sr^{2+}	MoO_4^-	Ag^+	Cd^{2+}	Cs^+	WO_4^-	Ba^{2+}	$PbCO_{3(s)}$	$UO_2(CO_3)_3^{4-}$

Table 4 : Proportion of dissolved trace elements in bulk waters (%). TE proportions are calculated dividing the TE content in the dissolved phase by the TE content in bulk waters. The symbol S1, S2 and S3 stand for the first, second and third sampling.

TE dissolved content (%)	Nature	Li	Al	Ti	Mn	Co	Cu	Zn	As	Rb	Sr	Mo	Ag	Cd	Cs	W	Ba	Pb	U
America S1	Waters draining mines	98	16	92	70	77	11	100	94	99	100	100	-	50	93	100	98	5	100
America S2		98	19	70	58	66	70	35	97	96	100	99	100	41	95	20	40	14	100
America S3		96	13	97	90	83	100	100	99	100	100	99	93	93	100	100	100	48	100
Pajaro Verde S1		83	-	100	8	100	-	100	100	97	100	100	-	91	100	98	100	10	96
Pajaro Verde S2		79	-	100	49	86	20	41	100	97	96	100	100	65	100	100	29	41	99
Pajaro Verde S3		45	26	64	76	33	46	26	100	99	99	38	100	66	100	44	99	97	100
Cruz Pintada S1	Drinking water	94	24	100	5	86	-	100	99	100	100	100	-	100	100	100	87	100	100
Cruz Pintada S2		100	11	47	84	66	89	15	88	86	100	99	100	100	37	4	15	14	65
Cruz Pintada S3		61	17	90	43	83	88	81	94	100	100	100	98	100	93	100	100	73	100
El Vivero S1		85	20	80	91	82	100	100	91	94	95	93	-	100	100	100	69	42	100
El Vivero S2		79	51	100	79	81	13	15	95	87	96	98	-	100	60	1	93	24	95
El Vivero S3		100	1	42	92	45	7	5	88	77	97	89	82	100	27	100	26	15	59
La Presita S1	Springs	83	-	100	100	76	100	100	100	93	100	77	-	100	100	77	96	100	94
La Presita S2		85	-	85	28	91	38	36	100	96	100	100	100	32	100	43	16	49	98
La Presita S3		84	33	88	69	99	51	22	88	97	98	96	94	-	98	99	86	92	99
Cascabeles S2		81	-	89	83	100	30	100	97	100	100	100	100	100	93	100	92	47	100
Cascabeles S3		71	40	86	53	100	57	74	93	96	99	99	98	100	96	85	95	83	95

Manantial Rio Nexpa S1		100	-	100	76	100	-	50	99	100	100	100	-	100	96	83	96	100	100
Rio Nexpa up S1	Riverwater	86	1	28	8	46	72	11	100	93	97	100	-	100	75	100	79	6	100
Rio Nexpa up S2		83	-	30	20	66	53	23	98	98	95	100	100	27	77	100	98	4	100
Rio Nexpa up S3		100	7	89	71	100	97	60	100	100	99	100	86	58	90	100	100	82	100
Rio Nexpa middle S1		87	4	34	24	59	98	46	97	95	100	100	-	25	72	100	86	10	100
Rio Nexpa middle S2		86	-	24	14	51	42	41	100	98	94	100	100	54	74	100	88	3	100
Rio Nexpa middle S3		100	1	70	56	92	88	57	99	97	99	97	73	58	86	100	97	64	100
Rio Nexpa down S1		98	1	23	13	33	34	14	90	92	92	100	-	100	56	100	71	3	100
Rio Nexpa down S2		86	-	26	19	65	46	25	99	98	95	136	100	56	79	356	27	10	100
Rio Nexpa down S3		100	0.4	42	25	84	62	28	95	97	98	100	73	64	79	100	96	57	100
Average (%)		**87**	**17**	**70**	**52**	**76**	**59**	**52**	**96**	**96**	**98**	**97**	**94**	**76**	**84**	**93**	**77**	**44**	**96**